Methods for the Assessment of Head-Mounted Displays in Visual Space

Yonggang Ha and Jannick Rolland
School of Optics / CREOL
University of Central Florida, Orlando FL
jannick@odalab.ucf.edu

ABSTRACT

Common techniques of lens design lead to image quality assessment in the plane of the miniature display of a head-mounted display (HMD) instead of image quality in visual space as expected from a usability point of view. In this paper, we present an analysis of HMD performance in visual space including MTF, accommodation, astigmatism, and transverse color smear.

Keywords: head-mounted displays; visual assessment; optical system design

1. INTRODUCTION

With the rapid development of virtual environment technology and wearable displays, the visual and human factor performance of head-mounted displays (HMDs) across multiple tasks is crucial. To this end, it is important to quantify the performance of the optics in visual space, given that visual metrics can then provide a baseline for usability and perception studies.[1-2]

Assessment in visual space requires first flipping the optical system,[3] so the lens can be raytraced backward. Furthermore, it requires computations based on the eye's visual acuity and depth of focus, itself a function of visual acuity and the size of the eye pupil. In this paper, the criteria presented for the optics of HMD assessment yields accurate performance directly in visual space, without approximations. The capability to perform exact computations rather than estimations is not only important but also efficient once macros are established.

2. METRICS IN VISUAL SPACE

All computations in visual space assume that the HMD optical system has been flipped. Generalized criteria for the assessment of the optics of HMDs in visual space include the MTF in cycles/arcmin, astigmatism and accommodation-shift in diopters, and transverse color smear in arcmin. Distortion, which changes sign when a lens is raytraced backward, is invariant in magnitude across spaces when expressed in percent.

2.1 MODULATION TRANSFER FUNCTION

For MTF assessment, the unit of spatial frequency should be converted from cycles per mm to cycles per arc minute (cycles/arcmin). The accurate computation of the MTF in cycles/arcmin engages the following steps summarized in Table 1. On the surface of the exit pupil where the eye will be located, a perfect lens is inserted to bring the image into focus. In the case of MTF computation, the only requirement for the perfect lens is that the effective focal length f' is such that 1 arc minute maps to 1 mm on the image plane of the perfect lens. Based on the imaging equation for a thin lens in air,[4] the focal length f' can be computed as

$$f' = \frac{1}{\tan\theta - \frac{1}{L}} \qquad (1)$$

Helmet- and Head-Mounted Displays VII, Clarence E. Rash, Colin E. Reese, Editors,
Proceedings of SPIE Vol. 4711 (2002) © 2002 SPIE · 0277-786X/02/$15.00

where θ equals 1 arc minute, and L is the virtual image distance of the HMD measured from the pupil of the eye. According to a sign convention where positive distances go from left to right, L takes on a negative value in Eq. (1). For the last step, we compute the MTF on the image plane of the perfect lens to yield directly the MTF in cycle/arcmin.

Table 1 Three steps to compute the MTF in visual space

Step	Description
1	Insert a perfect lens in the exit pupil to bring the image into focus.
2	Set the correct focal length of the perfect lens to insure that 1 arcmin maps
3	Compute the MTF on the image plane of the perfect lens.

2.2 ASTIGMATISM AND ACCOMMODATION-SHIFT

Given a point in the field of views (FOV), astigmatism is measured as the difference in vergence between the sagittal and the tangential components of a small beam of light around the chief ray. The minimum resolution loss due to astigmatism can be defined by choosing a focus plane one-half way between the sagittal and the tangential foci. In visual space this plane corresponds to a shift in accommodation (i.e. referred as accommodation-shift thereafter) from the nominal virtual image plane. Accommodation-shift is thus measured as the difference in vergence between the nominal virtual image point and the midpoint between the sagittal and tangential images of that point.

When astigmatism is measured conventionally in the space of the miniature LCD, astigmatism is either measured as the distance between the sagittal and tangential foci in mm or as the length of the lines formed on the tangential or sagittal surfaces in mm. In visual space, astigmatism is best evaluated in diopters for the longitudinal component or arc minutes for the transverse component. An object distance D_{Lm} expressed in diopters is defined as the inverse of the distance L_m expressed in meters. D_{Lm} has a positive value when the object is in front of the eye, or equivalently the light entering the eye pupil is divergent. If D_{Lm} is negative, the light entering the eye is convergent, and most people cannot bring the image into focus.

Given a virtual image presented in a HMD, objects can be perceived sharply around the nominal virtual screen distance where the eyes are focused, given the depth of focus and corresponding depth of field of the human visual system. Let's denote, O_D and O_P the distal and proximal planes that define the depth of field, L_D and L_P the distances of these two planes from the eye, and L_O the nominal focusing distance all represented in Fig.1. The depth of field is determined by the visual acuity angle η also shown in Fig. 1 and the diameter d of the eye pupil. The acuity angle η is defined either by the resolution in visual space as set by the angular subtends of a pixel or by the human visual system acuity. It is important to assess the optics with respect to the human visual system acuity as well given that higher resolution miniature displays are constantly becoming commercially available.

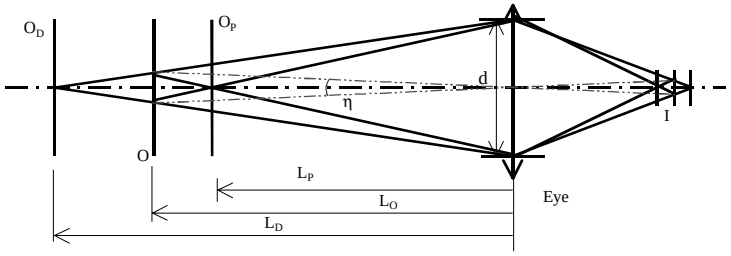

Fig.1 Schematic layout of imaging of the eye and the corresponding depth of field

The larger η, the larger the depth of field, but the lower the achievable resolution. The distances L_D and L_P expressed in diopters are given by

$$D_D = \frac{1}{-L_D} = -\frac{d + \eta L_O}{L_O d}$$
$$D_P = \frac{1}{-L_p} = -\frac{d - \eta L_O}{L_O d} \quad , \tag{2}$$

where d and L_O are expressed in meters and η in radians. Objects outside the depth of field will be seen more blurred than at L_O unless the user refocuses, and optical aberrations that extend outside this range would contribute to a loss in resolution. This concept was used to develop multifocal planes HMDs.[6]

In visual space, astigmatism and accommodation-shift across the FOV can be computed according to the steps summarized in Table 2. A perfect lens is added in the exit pupil where the eye will be located. The perfect lens should simulate an average human eye insofar as the focal length is concerned (i.e. f'=17 mm). Furthermore, the size of the exit pupil should be set to a value corresponding to low levels of illumination (i.e. a 3 mm pupil diameter is employed in the computations presented thereafter). The pupil size and focal length together set the depth of focus and the corresponding depth of field of the human eye given by Eq. (2), which is utilized to set a tolerance on acceptable astigmatism and accommodation-shift for the design. We then trace sagittal and tangential rays to the image plane of the perfect lens with a small aperture value (i.e. close skew rays) around the chief ray in order to obtain the focus locations of the sagittal and tangential rays across the FOV, respectively. With non-rotationally symmetric systems, rays in XZ and YZ sections are traced instead.[7,8] Also the average values of the sagittal and tangential defocus values with respect to the paraxial image plane position are computed. The defocus values are expressed in diopters as follows

$$D = -\left(\frac{1}{L' + \Delta} - \frac{1}{f'}\right) \quad , \tag{3}$$

where L' is the paraxial image distance behind the perfect lens, Δ is the defocus values for astigmatism or the average defocus values for accommodation-shift, and f' is the focal length of the perfect lens.

Table 2 Ten steps to compute astigmatism and accommodation-shift in visual space

Step	Description
1	Add a perfect lens with an aperture size equivalent to the pupil of the eye (depends on illumination) in order to bring the image into focus.
2	Trace rays and get the sagittal and tangential foci across the FOV.
3	Compute the sagittal and the tangential defocus values and well as their averages with respect to the paraxial image plane.
4	Convert all defocus values to diopters.
5	Compute the diopter range for the depth of field and eliminate the diopter values outside the depth of field.
6	Compute the difference between the sagittal and the tangential diopter values for astigmatism.
7	Compute the difference between the average diopter value and the nominal diopter value for accommodation-shift.
8	Print 2D data tables of astigmatism and accommodation-shift values as a function of the FOV and draw 2D plots accordingly.
9	Print 2D data tables of astigmatism in arc minutes as a function of the FOV and draw a 2D plot accordingly showing astigmatism greater than 1 arc minute

The diopter values *D* that fall outside the depth of field are eliminated in the final graphical representation of the performance by setting a dot at the respective points in the FOV. Results of the computation are presented as a 2D data table of retained astigmatism and accommodation-shift values as a function of the FOV and as a 2D plot.

2.3 TRANSVERSE COLOR SMEAR

For HMDs with color capability, transverse color smear can limit image quality and must be assessed. In visual space, transverse color smear will be measured in arc minutes. Two kinds of transverse chromatic aberrations will be assessed: transverse lateral color and transverse secondary color. Transverse lateral color is the chief ray location difference of the two outer wavelengths measured in arc minutes over the FOV. For the visible spectrum, the outer wavelengths are usually C and F. For those optical systems corrected in lateral color for C and F wavelengths, the residual chromatic smear is from secondary color, which is defined by the chief ray location difference of the reference wavelength and the common point of the two outer wavelengths. Thus, transverse chromatic aberrations in visual space are computed according to the steps summarized in Table 3. Let's denote the coordinates of the chief rays of the outer wavelengths on the image plane as (X_C, Y_C) and (X_F, Y_F), and the coordinates of the chief ray for the reference wavelength as (X_R, Y_R). The transverse lateral color (TLC) and the transverse secondary color (TSC) expressed in arc minutes are computed using Eq. (4) and (5) given by

$$TLC = \left(\tan^{-1}\left(\frac{\sqrt{X_C^2 + Y_C^2}}{L'} \right) - \tan^{-1}\left(\frac{\sqrt{X_F^2 + Y_F^2}}{L'} \right) \right) \times \frac{180 \times 60}{\pi} \quad , \tag{4}$$

$$TSC = \left(\tan^{-1}\left(\frac{\sqrt{X_R^2 + Y_R^2}}{L'} \right) - \tan^{-1}\left(\frac{\sqrt{\left(\frac{X_C + X_F}{2} \right)^2 + \left(\frac{Y_C + Y_F}{2} \right)^2}}{L'} \right) \right) \times \frac{180 \times 60}{\pi} \quad , \tag{5}$$

where L' is the paraxial image distance. The results are similarly presented in the form of 2D data tables and 2D plots.

Table 3 Four steps to compute transverse color smear in visual space

Step	Description
1	Add a perfect lens with appropriate aperture size to bring the image into focus.
2	Across the FOV, trace chief rays of the outer wavelengths and the reference wavelength to the image plane behind the perfect lens.
3	Compute transverse lateral color and transverse secondary color in visual space in term of arc minutes based on ray tracing.
4	Print 2D data tables of aberration versus FOV and draw 2D plots accordingly.

3. APPLICATION OF THE METHODS TO AN ERFLE EYEPIECE

In order to validate the framework presented, we implemented the methods detailed in this paper in several macro files written in this specific case, but with no loss of generality, with CODE V® (software from Optical Research Associates, Pasadena, California). These macros are made accessible on the web at http://odalab.ucf.edu/macro and are written in ASCII format. The various macros developed are listed in Table 4.

Because eyepiece optics is often employed in HMD designs, we chose an Erfle eyepiece as an example. An off-axis example assessed via an earlier version of the methods is provided in Rolland (2000).[3] Table 5 provides the design specification of the eyepiece, and Table 6 the optimized prescription data. The schematic design layout is provided in Fig.2. To demonstrate the generalization of the assessment methods, we set different values of the FOVs in both the X

and Y directions.[7] Fig.3 and Fig. 4 show assessments of distortion and MTF evaluated on the LCD plane of the HMD. Fig. 5 shows the layout of the optical system after flipping of the optics and insertion in the pupil of a perfect lens.

Table 4 List of available macro files at http://odalab.ucf.edu/macro

File name	Function
VSFlip.seq	Performs flip of optical systems, adds perfect lens, and sets the pupil size to the user's request.
VSMTF.seq	Computes MTF as a function of spatial frequency in cycles/arcmin and output data table and plot.
VSTCS.seq	Computes transverse color smear in arcmin, including transverse lateral color and secondary lateral color, and output data tables
VSACAS.seq	Computes accommodation and astigmatism in diopters and output data tables and plots.

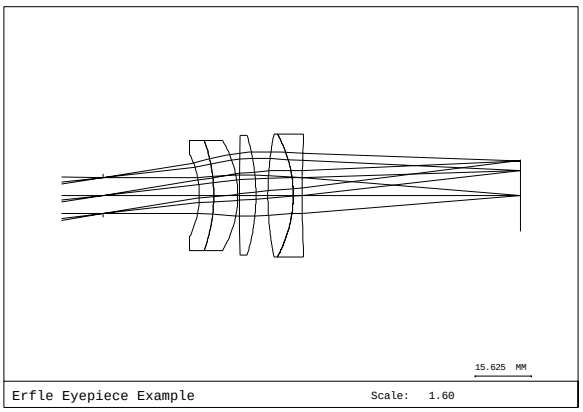

Fig.2 2D Layout of the Erfle eyepiece

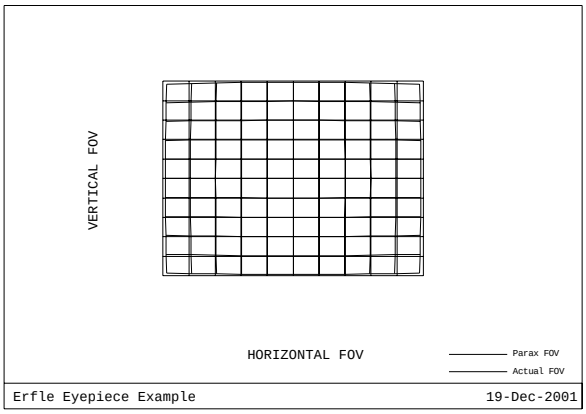

Fig.3 Distortion of the Erfle eyepiece

Table 5 Design Specification

Parameter	Specification
Object: Color LCD	
a. Size	1.3 inch diagonal
b. Active display area	Rectangular, 26.4mm x 19.8mm
c. Resolution	800 x 600 pixels
Eyepiece:	
a. Type	Erfle eyepiece
b. Effective focal length	61.6 mm
c. Exit pupil diameter	10 mm
d. Virtual image distance	2 m from the eye pupil
e. Eye relief	25 mm
Other parameters:	
Wavelength range	656 to 486 nm
FOV	30° in diagonal
Distortion	<5% over entire FOV

Table 6 Prescription data for the Erfle eyepiece

Surface number	Radii	Thickness	Glass
Object	Infinity	-2000.00	AIR
1(Stop)	Infinity	26.55	AIR
2	-25.9	3.98	F2
3	-45.36	6.65	BK7
4	-29.64	0.50	AIR
5	2323.16	4.51	SSK1
6	-57.70	3.31	AIR
7	86.722	7.00	SK4
8	-35.57	2.50	SF12
9	343.63	60.30	AIR
Image	Infinity	0.00	

To assess the MTF in visual space, we applied the macro file VSMTF.seq with the flipped system. Based on Eq. (1), the focal length of the perfect length at the stop surface is set to 1264.40 mm in order to yield the MTF with spatial frequency in unit of cycles/arcmin. The result of MTF in visual space is shown as in Fig. 6.

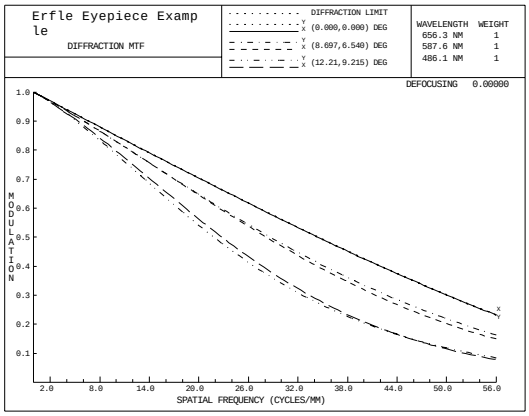

Fig.4 Polychromatic MTF in cycles/mm with a 3-mm pupil

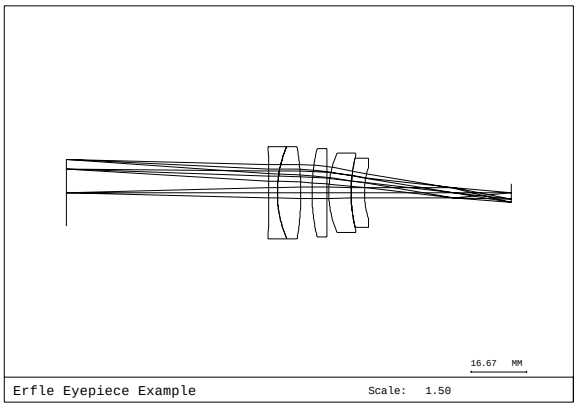

Fig.5 2D layout of the Erfle eyepiece after inversion and insertion of a perfect lens in the pupil

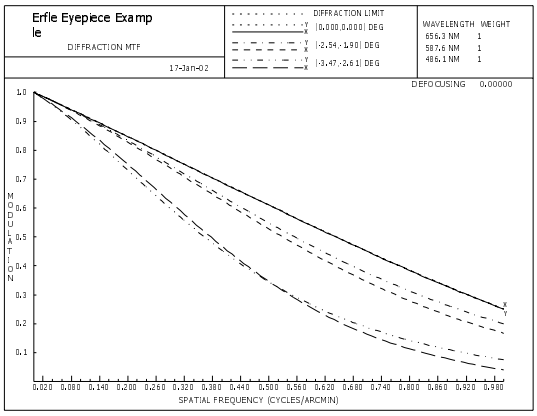

Fig. 6 Polychromatic MTF for a 3-mm pupil as a function of the spatial frequency in cycle/arcmin

Accommodation-shift and astigmatism in visual space were assessed with the macros VSACAS.seq. Given a 3 mm pupil and a resolution angle of 1 arc minute, the depth of field ranges from 0.403 to 0.597 diopters. Accommodation-shift expressed in diopters as a function of the FOV is shown in Fig. 7. Astigmatism expressed in diopters as a function of the FOV is shown in Fig. 8. The diameter of the circles in the plots is proportional to the magnitude of accommodation-shift and astigmatism measured in diopters.

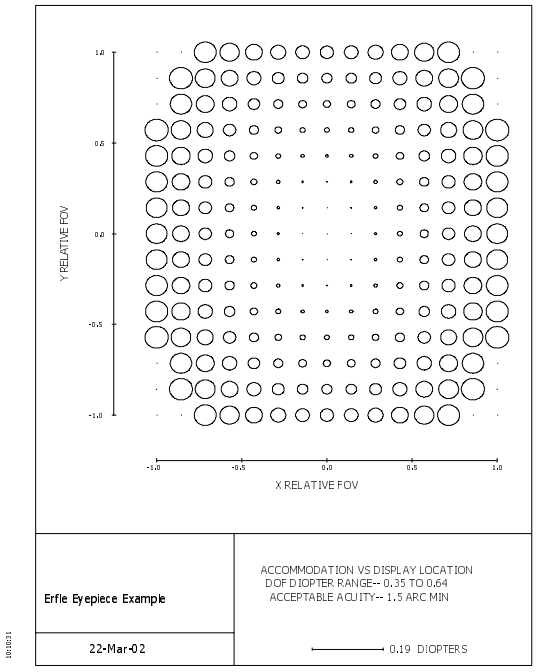

Fig.7 Accommodation-shift in diopters for a centered 3-mm pupil

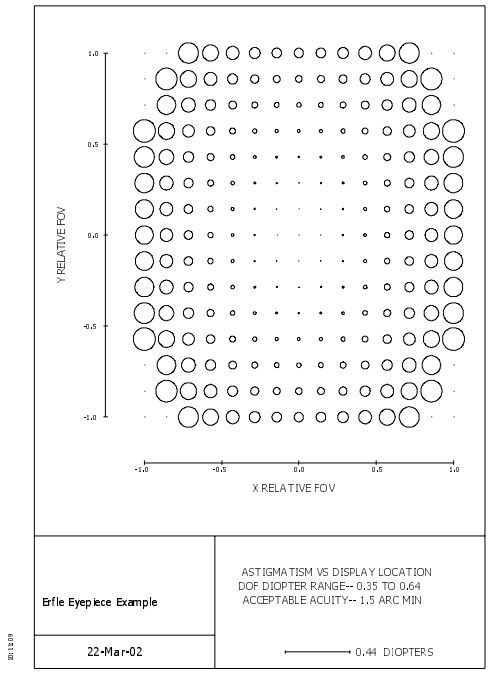

Fig.8 Astigmatism in diopters for a centered 3-mm pupil

Results show that both accommodation-shift and astigmatism are within the specified visual performance of the system for 80 percent of the FOV. Therefore, all points within 80 percent of the FOV will be perceived as sharp points when the eyes accommodate in the plane of the virtual image provided. Furthermore, if the visual angle subtended by the pixels of the miniature display is larger than 1 arc minute, the pixels will be resolvable and in the case of residual astigmatism will appear elongated as well.

Finally, applying the macro file VSTCS.seq to the flipped eyepiece, we computed the transverse lateral color and secondary color smear in arc minutes. Fig. 9 shows the transverse lateral color versus FOV for a centered 3 mm pupil, and Fig. 10 provides the corresponding plot for secondary color smear. Results show that the design is not limited by either aberration given that all circles are less than 1 arc minute and therefore the color smear will not be resolved. This analysis can naturally be extended to decenters of the pupil.

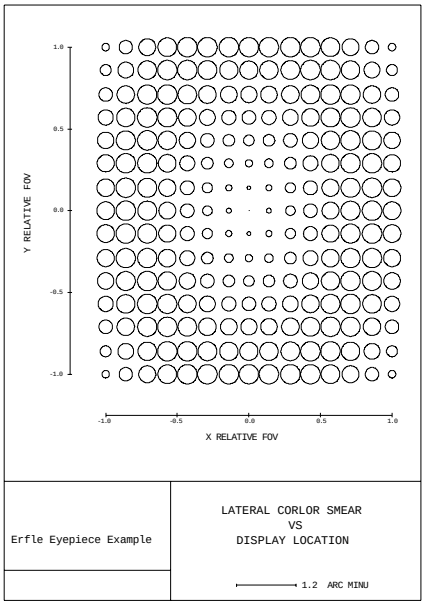

Fig. 9 Transverse lateral color in arcmin

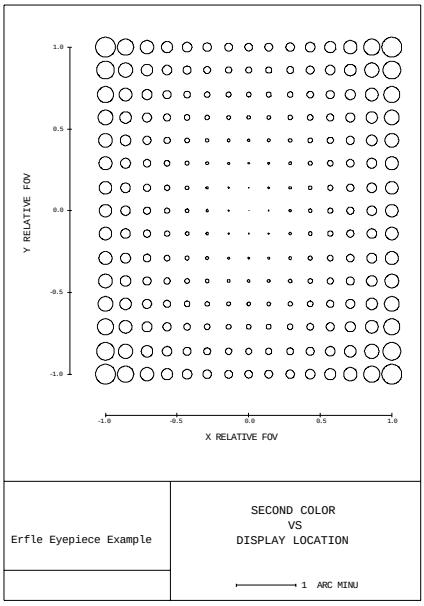

Fig. 10 Transverse secondary color in arcmin

4. CONCLUSION

The image quality in HMDs can be easily assessed in visual space. MTF performance is directly provided in cycles/arcmin, accommodation-shift and astigmatism in diopters, and transverse color smear is arc minutes. Assessment of HMD performance in visual space provides not only direct information about perceived image quality, it will also surely help bridge the gap between optical design engineers and experts in the visual and human factor assessment of the technology.

5. ACKNOWLEDGEMENTS

We thank Martin Shenker for inspiring this research, and Kevin Thompson and John Isenberg from Optical Research Associates for their assistance with the development of some earlier version of the macro files provided and some access to internal code related to computation of astigmatism line length, respectively. Finally we thank Hong Hua for stimulating discussions about this research. This research is supported by the NIH/NLM 1-R29-LM06322-01A1, the NSF IIS 00-82016 ITR and EIA-99-86051.

REFERENCES

1. Rolland, J. P., D. Ariely, and W. Gibson, "Towards quantifying depth and size perception in virtual environments," Presence: Teleoperators and Virtual Environments (MIT Press), 4(1), 24-49 (1995).
2. M. Shenker, "Image quality considerations for head-mounted displays," in OSA Proceedings of the International Optical Design Conference 22, G. W. Forbes, Ed., pp. 334-338 (1994).
3. J.P. Rolland, "Wide-angle, off-axis, see-through head-mounted display," Optical Engineering 39(7), 1760-1767 (2000).
4. P. Mouroulis and J. Macdonald, Geometrical Optics and Optical Design, Oxford University Press, (1997).
5. J.P. Rolland, V. Shaoulov, and F.J. Gonzalez, "The art of back-of-the-envelope paraxial raytracing," IEEE Transactions in Education, 44, 365-372 (2001).
6. J.P. Rolland, M. W. Krueger, and A. Goon, "Multifocal planes head-mounted displays," Applied Optics 39(19), 3209-3215 (2000).
7. K.P. Thompson, "Aberration fields in nonsymmetric optical systems," PHD Dissertation, University of Arizona (1980).
8. J.R. Rogers, "Techniques and tools for obtaining symmetrical performance from tilted-component systems," Optical Engineering 39(7), 1776-1787 (2000).